# Efficiencies of Electron Injection from Excited N3 Dye into Nanocrystalline Semiconductor ($ZrO_2$, $TiO_2$, ZnO, $Nb_2O_5$, $SnO_2$, $In_2O_3$) Films

**Ryuzi Katoh,*,† Akihiro Furube,† Toshitada Yoshihara,† Kohjiro Hara,† Gaku Fujihashi,‡ Shingo Takano,‡ Shigeo Murata,† Hironori Arakawa,† and M. Tachiya§**

*Photoreaction Control Research Center (PCRC), National Institute of Advanced Industrial Science and Technology (AIST), AIST Tsukuba Central 5, Tsukuba, Ibaraki 305-8565, Japan, and Sumitomo Osaka Cement Co., Ltd., 585 Toyotomi, Funabashi, Chiba 274-8601, Japan*

*Received: November 20, 2003*

The efficiency of electron injection from excited N3 dye (*cis*-bis-(4,4′-dicarboxy-2,2′-bipyridine) dithiocyanato ruthenium(II), $Ru(dcbpy)_2(NCS)_2$), into various nanocrystalline semiconductor ($ZrO_2$, $TiO_2$, ZnO, $Nb_2O_5$, $SnO_2$, $In_2O_3$) films was studied by transient absorption spectroscopy. For $TiO_2$, ZnO, $Nb_2O_5$, $SnO_2$, or $In_2O_3$ films, injection efficiencies were found to be very high; for $ZrO_2$ film, the efficiency was very low. These findings indicate that electron injection occurs efficiently if the LUMO level of N3 dye is located sufficiently far above the bottom of the conduction band of the semiconductor film. On the basis of the results, we discuss the reason $TiO_2$ exhibits higher solar cell performance than other materials.

## Introduction

In 1993, Grätzel and co-workers developed a highly efficient dye-sensitized solar cell consisting of N3 dye (*cis*-bis-(4,4′-dicarboxy-2,2′-bipyridine) dithiocyanato ruthenium(II), $Ru(dcbpy)_2(NCS)_2$), adsorbed on nanocrystalline $TiO_2$ film. The solar-energy-to-electricity conversion efficiency $\eta$ of the cell was 10% under AM 1.5 irradiation.[1] In the past decade, considerable efforts have been made to improve the performance of such solar cells, but without much success. Many sensitizing dyes have been synthesized, and many methods for preparing nanocrystalline films have been examined.[2,3]

The type of materials of the nanocrystalline films is also an important parameter, so other materials, such as ZnO, $SnO_2$, and $Nb_2O_5$ have been tested. Arakawa and co-workers studied solar cell performance in various materials.[4,5] The short circuit current $J_{SC}$ was measured, and the solar cell using $TiO_2$ films exhibited an exceptionally high $J_{SC}$. Hagfeldt and co-workers have studied dye-sensitized solar cells based on nanocrystalline ZnO films.[6] They found that the photocurrent decreases with increasing concentration of N3 dyes adsorbed on the surface because of the formation of complexes between the N3 dyes and $Zn^{2+}$ ions on the surface.[6] We also studied the complex formation and found that the complexes form micrometer-sized crystals on the surface.[7] The aggregation can be suppressed by changing the countercation of N3 dyes from $H^+$ to tetrabutylammonium (TBA),[6] resulting in a marked improvement in solar cell performance ($\eta = 5\%$).[8] Noteworthy is the fact that, despite many attempts to improve it, the solar cell performance for ZnO films remains lower than that of the $TiO_2$ system. These facts imply that some properties of the $TiO_2$ films are important to achieve high solar cell performance.

The detailed operating mechanism of these solar cells has been studied extensively to identify the processes that limit their performance. Figure 1 illustrates the primary processes of dye-sensitized solar cells. The balance of these processes is important to achieve high performance. Upon photoexcitation of the sensitizer dye, the electrons are injected from the excited sensitizer dyes into the conduction band (CB) of the semiconductor film (electron injection). The injected electrons recombine with the oxidized sensitizer dyes (recombination). This recombination process competes with the regeneration of the oxidized sensitizer dyes by the redox mediator molecules (regeneration). The remaining electrons can be transported in the semiconductor film as the conducting electrons. The conducting electrons can react with the redox mediator molecules or with molecules in the solution during transport, before reaching the back contact electrode (leak reaction). Finally, the remaining electrons flow into the external circuit. The rate and efficiency of these processes depend strongly on the nature of the sensitizer dye and semiconductor film.

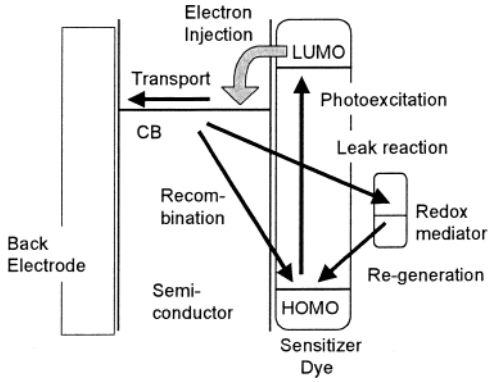


**Figure 1.** Primary reaction processes in dye-sensitized solar cells.

As shown in Figure 1, there are several primary processes in dye-sensitized solar cells. To explore the processes that limit their performance, many studies have been carried out. Transient absorption spectroscopy is one of the most powerful tools to study these processes, especially the electron injection process. Although there have been many studies making use of a

* Corresponding author. E-mail: r-katoh@aist.go.jp.
† PCRC, AIST.
‡ Sumitomo Osaka Cement Co., Ltd.
§ AIST.

10.1021/jp031260g CCC: $27.50 
Published on Web 03/23/2004

femtosecond pulsed laser, only a few studies have attempted to clarify the difference in semiconductor properties. Lian and co-workers determined the rate of electron injection from excited N3 dyes into $TiO_2$, $SnO_2$, and ZnO films by observing the change in infrared absorption caused by the production of conducting electrons.[9] According to their study, ultrafast electron injection (<100 fs) occurs in $TiO_2$, whereas relatively slow injection (on the picosecond time scale) is found in $SnO_2$ and ZnO systems. They pointed out that this is due to the difference in the density of states of the conduction band. For $SnO_2$, the injection dynamics was also studied and it was found that the injection dynamics is multiexponential, including components ranging from very fast (<100 fs) to slow ones (>1 ps).[10−12] Recently, by observing the absorption in the near-infrared wavelength range, we found that stepwise injection through exciplex-like intermediates occurs in the N3/ZnO system, whereas very fast direct injection occurs in the N3/$TiO_2$ system.[13] Clearly, the electron injection dynamics differs among materials.

The rate of electron injection is very fast, suggesting that the efficiency of electron injection is very high. However, fast injection dynamics does not necessarily lead to a high efficiency of electron injection. This is because, in some cases, sensitizer dye becomes inactive for electron injection due to unfavorable adsorption geometry. To evaluate the electron injection efficiency directly, we have used nano-second transient absorption spectroscopy.[7,14,15] The relative efficiency of electron injection can be evaluated from the absorbance of conducting electrons or of oxidized forms of sensitizer dyes, when all measurements are made under the same optical geometry through transient absorption measurements. We measured the relative injection efficiency for derivatives of Ru−phenanthroline complexes adsorbed on $TiO_2$ films and found that a molecule having one carboxyl group exhibited a very low efficiency compared with a molecule having four carboxyl groups.[14] From the analysis of transient absorption signal, we conclude that there are two modes of adsorption of the molecule on $TiO_2$ surface, one is active for the injection and the other is inactive. We also studied the formation of inactive molecular aggregates.[7] For N3 dyes adsorbed on ZnO, we observed the formation of micrometer-sized crystals of a complex between N3 and $Zn^{2+}$, which were inactive for electron injection. It should be noted that direct measurements of the efficiency of electron injection is important to study the electron injection process of dye-sensitized solar cells.

Here we evaluate the efficiency of electron injection from excited N3 into various nanocrystalline semiconductor films ($ZrO_2$, $TiO_2$, ZnO, $Nb_2O_5$, $SnO_2$, $In_2O_3$). On the basis of the results, we discuss the reason $TiO_2$ exhibits higher solar cell performance than other materials.

## Experimental Section

$TiO_2$ nanoparticles were prepared by the method reported by Grätzel and co-workers.[16] Commercially available ZnO, $Nb_2O_5$, and $ZrO_2$ powders (Sumitomo Osaka Cement Co. Ltd.) were used. Nanoparticles of $SnO_2$ and $In_2O_3$ were synthesized by calcination of the corresponding hydroxides, produced by precipitation through adjustment of the pH of $SnCl_4$ and $In(NO_3)_3$ solutions with $NH_3$. An organic paste containing the semiconductor nanoparticles was printed onto a glass substrate by a screen-printing technique, as reported elsewhere.[17] The films obtained had an area of 1 $cm^2$ (1 cm × 1 cm) and thickness of 2−5 $\mu$m. The N3 dye (Solaronix SA) was used without purification, and was dissolved in a 50:50 solution of *tert*-butyl alcohol (Kanto Chemical) and acetonitrile (Kanto Chemical, dehydrated) to give a 0.3 mM solution. The semiconductor ($ZrO_2$, $TiO_2$, $Nb_2O_5$, $SnO_2$, $In_2O_3$) films were immersed in the dye solution, and then kept at 25 °C for over 10 h so that the dye could be adsorbed onto the semiconductor surface. For ZnO films, it has been reported that the formation of a complex between N3 dyes and $Zn^{2+}$ ions occurs during immersion.[7] Therefore, the sample specimens were immersed in the dye solution for less than 1 h at 25 °C to minimize complex formation on the ZnO films. The sample specimens were dried in air and used for transient absorption measurements. All measurements were carried out just after the preparation of the sample specimens to minimize the effect of dye degradation.

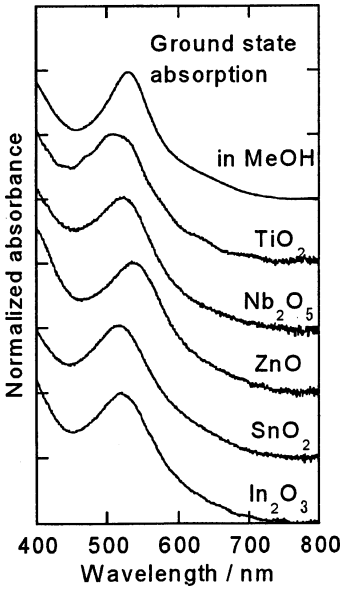


**Figure 2.** Absorption spectra of N3 dye adsorbed on various semiconductor films normalized at a peak.

Absorption spectra were measured with an absorption spectrophotometer (Shimadzu, UV-3101PC). Light transmitted through a sample specimen was corrected by an integrating sphere to minimize the artifact due to light scattering by the substrate. For the transient absorption measurements, the second harmonic pulse (532 nm) from a $Nd^{3+}$:YAG laser (Continuum, Surelite II) was used for pumping light. The duration of the laser pulse was 8 ns. A Xe flash lamp (Hamamatsu, L4642, 2 $\mu$s pulse duration) was used as a probe light source. The probe light was focused on a sample specimen (2 mm in diameter). The area probed by the probe light was covered by that irradiated with the exciting light (10 mm in diameter). All measurements were carried out under the same optical geometry to obtain the relative efficiencies of electron injection. The probe light transmitted through the sample specimen was detected with a Si-photodiode (Hamamatsu, S-1722) after being dispersed with a monochromator (Ritsu, MC-10N). Signals from the photodetector were processed with a digital oscilloscope (Tektronix, TDS680C) and were analyzed with a computer. The intensity of the laser pulse was measured with a pyroelectric energy meter (Gentec, ED-200L). All measurements were carried out at 295 K.

## Results and Discussion

**Absorption Spectra of N3 Dyes Adsorbed on Various Semiconductor Films.** Figure 2 shows absorption spectra of N3 dye adsorbed on various nanocrystalline semiconductor films together with that in solution normalized at a peak. Actual

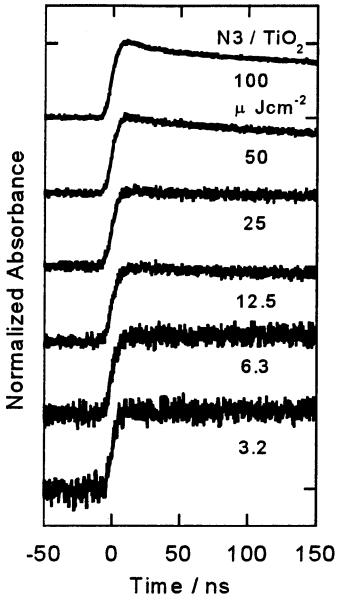


**Figure 3.** Temporal profiles of transient absorption observed at 800 nm in N3/$TiO_2$ at various exciting light intensities.

absorbance of these specimens is about 0.2−0.4 at the peak. These spectra are similar to that in solution which is assigned to metal-to-ligand charge-transfer transition.[18] This suggests that the interaction between N3 dye and the semiconductor films in the ground state is weak. Strictly speaking, the peak position differs slightly between materials. This difference may reflect differences in the interaction.

**Transient Absorption Spectra of Oxidized N3 Dyes on Various Semiconductor Films.** Figure 3 shows the decay profiles of the transient absorption signals of N3 dye adsorbed on nanocrystalline $TiO_2$ film, (abbreviated as N3/$TiO_2$) at 800 nm for various excitation intensities. The oxidized state of the N3 dye is observed at this wavelength.[19] The transient absorption signal grows within the time resolution of the measurement system (10 ns), suggesting that charge separation occurs immediately upon photoexcitation of N3 dyes. The decay of the signal is due to charge recombination. For a higher excitation intensity ($>50\ \mu J\ cm^{-2}$), a faster decay is seen. This is consistent with a previous observation reported by Durrant and co-workers.[20] According to their interpretation, the faster decay is due to the acceleration of charge recombination by the trap-filling effect.[20,21] At lower excitation intensities ($<25\ \mu J\ cm^{-2}$), no decay of the signals can be observed in the time range recorded, suggesting that the charge recombination is very slow under these excitation conditions.

The amplitude of the transient absorption signal shown in Figure 3 is proportional to the number of electrons remaining in the nanocrystalline films. Thus, the relative efficiencies of electron injection can be obtained from the absorbance at 0 ns, and these are plotted as a function of excitation intensity in Figure 4. In the case of lower excitation intensities, the efficiency is constant, whereas it decreases with increasing light intensities at higher excitation intensities. At present, the reason is unclear, and two possible reasons can be considered for the suppression. One is fast recombination due to the trap-filling effect, and the other is the energy shift of the conduction band of the semiconductor film induced by the accumulation of electrons.

Figure 5 shows the transient absorption signals of N3 dyes adsorbed on various nanocrystalline semiconductor ($TiO_2$, ZnO, $Nb_2O_5$, $SnO_2$, $In_2O_3$) films observed at 800 nm under a sufficiently low excitation intensity condition ($<20\ \mu J\ cm^{-2}$).

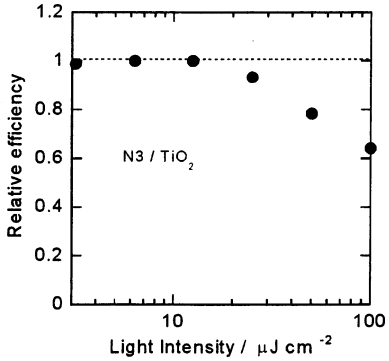


**Figure 4.** Relative efficiencies of electron injection of N3/$TiO_2$ as a function of the intensities of the exciting light.

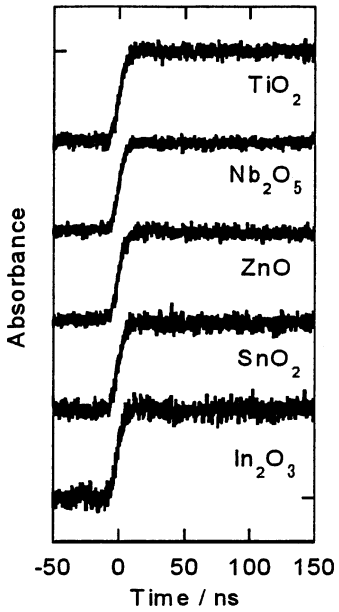


**Figure 5.** Temporal profiles of transient absorption of various systems observed at 800 nm.

Obviously, the signals grow within the time resolution of our apparatus (10 ns), and are then constant over the remainder of the time range recorded. Figure 6 shows the transient absorption spectra in these systems. All the spectra have a peak at around 800 nm, suggesting the presence of the oxidized form ($N3^+$) of N3 dye on the surface.[19] The decay profiles at all wavelengths of the transient spectra are similar to those at 800 nm shown in Figure 5. This indicates that the absorption spectrum of excited dye does not overlap with that of oxidized N3 dye. Strictly speaking, the spectral shape of $N3^+$ differs slightly between materials. This difference in the spectral shape may reflect differences in the interaction between the N3 dye and the semiconductor films.

We also measured the transient absorption of N3/$ZrO_2$. Excited N3 dyes on $ZrO_2$ films cannot inject electrons into the conduction band because the energy of the bottom of the conduction band of $ZrO_2$ is considerably higher than the LUMO level of N3 dye. Figure 7 shows the transient absorption signal of N3/$ZrO_2$ recorded at 800 nm. In contrast to the other semiconductor films shown in Figure 5, the transient absorption signal decays rapidly. As shown in Figure 7, the decay profile of the transient absorption is similar to that of fluorescence (solid line) from N3 dyes in the film, as well as that in solution (25 ns).[19] This indicates that excited N3 dyes on $ZrO_2$ films decay without electron injection into the films. Thus, it is considered that the transient absorption signal is not due to the oxidized

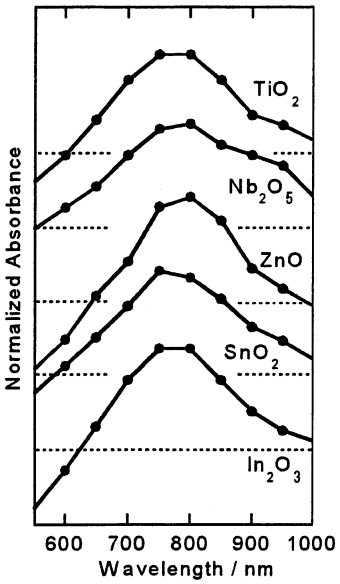


**Figure 6.** Transient absorption spectra of N3 adsorbed on various semiconductor films.

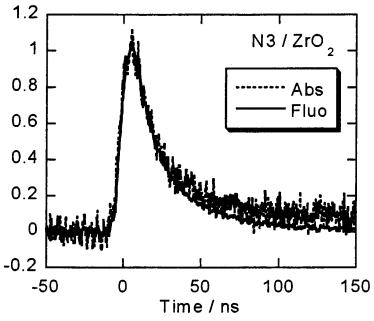


**Figure 7.** Temporal profiles of transient absorption observed at 800 nm (dashed line) and fluorescence at 800 nm (solid line) in N3/$ZrO_2$.

form of N3 dye but is due to the excited state of the N3 dye. Strictly speaking, the transient absorption signal does not decay completely over a longer time range. This implies that a small amount of the excited N3 dyes undergo charge separation.

**Efficiency of Electron Injection.** In a previous paper, we estimated the relative injection efficiency $\Phi_{inj}^{rel}$, from the absorbance change $A_{ox}$ of the oxidized N3 dye ($N3^+$), absorbance $A$ at the wavelength of exciting light and the intensity $I_{ex}$ of exciting light,[7,14,15]

$$\Phi_{inj}^{rel} = \frac{A_{OX}}{(1 - 10^{-A})I_{ex}} \quad (1)$$

The same procedure can be applied to the present study; however, the spectrum of $N3^+$ differs slightly among the semiconductor films. To evaluate the number of $N3^+$ generated, we use the integrated intensity $S_{ox}$ of the absorption spectra of $N3^+$ in the wavelength from 600 to 1000 nm,

$$\Phi_{inj}^{rel} = \frac{S_{OX}}{(1 - 10^{-A})I_{ex}} \quad (2)$$

Recently, we estimated that the absolute value of the electron injection efficiency in the N3/ZnO system is $0.95 \pm 0.15$.[22] By using this absolute value, one can estimate the injection efficiency as a function of the free energy change $\Delta G$ for the electron injection (Figure 8).

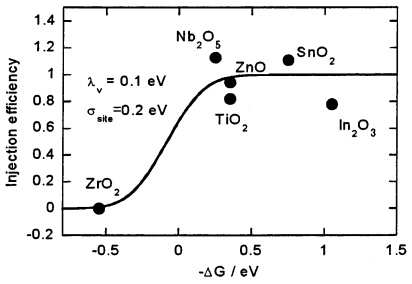


**Figure 8.** Relative efficiency of the electron injection as a function of $-\Delta G$. The solid line shows the results based on the model presented previously with the values of $\lambda_v = 0.1$ eV and $\sigma_{site} = 0.2$ eV.

The free energy change $\Delta G$ is expressed as

$$-\Delta G = -e(E_{OX}^{dye*} - E_{CB}) \quad (3)$$

where $E_{CB}$ is the reduction potential of the conduction band of the semiconductor film, and $E_{OX}^{dye*}$ is the oxidation potential of N3 dye in the excited state. It is difficult to determined $E_{CB}$ precisely, because it is sensitive to the surface condition and pH of solutions. Nevertheless, the $E_{CB}$ values of materials have been reported by several groups[2,4] and we simply used the values of $ZrO_2 = -1.4$ V, $TiO_2 = -0.5$ V, ZnO $= -0.5$ V, $Nb_2O_5 = -0.6$ eV, $SnO_2 = -0.1$ V, $In_2O_3 = 0.2$ V (vs NHE, pH = 7).

To evaluate the $E_{OX}^{dye*}$, we assume that electron injection occurs after relaxation. Given this condition, $E_{OX}^{dye*}$ is expressed as

$$eE_{OX}^{dye*} = eE_{OX}^{dye} - E_{0-0} \quad (4)$$

where $E_{0-0}$ is the energy difference between the ground state and the relaxed excited state. In the case of the Ru-complex, intersystem crossing from the singlet excited state (Franck−Condon state) to the triplet excited state is known to be very fast.[23] Therefore, the onset energy of the emission from the triplet state, reported to be 1.91 eV,[18] is used as the value for $E_{0-0}$. $E_{OX}^{dye}$ is reported to be 1.06 V (vs NHE),[18] so $E_{OX}^{dye*}$ can be estimated as 0.85 eV (vs NHE).

Recently, electron injection from unrelaxed excited states has been observed in $TiO_2$[24] and $SnO_2$ systems[10−12] as one of electron injection paths. For this reaction path, the photon energy of the exciting light should be used as the value of $E_{0-0}$ in eq 4.[15] In the present study, we used 532-nm light ($h\nu = 2.33$ eV) for excitation, so that all data points in Figure 8 should be shifted by 0.42 eV in the positive direction, under this assumption. However, at present, the contribution of the ultrafast injection path is not clear, and therefore we assume that electron injection occurs dominantly after the relaxation; i.e., we take the lowest value of $-\Delta G$.

As shown in Figure 8, the injection efficiencies of the systems having positive $-\Delta G$ values are very high, and not sensitive to the values of $-\Delta G$. This indicates that there are few dyes inactive for electron injection in these systems; i.e., almost all excited states undergo electron injection. For the N3/ZnO system, we previously found that N3 dyes form aggregates with $Zn^{2+}$ ions, and the aggregates are inactive for electron injection.[7] In the present study, we prepared sample specimens carefully by immersing the ZnO films in N3 solution for less than 1 h. Under these conditions, aggregation can be ruled out.[7]

We recently presented a model for electron injection of excited molecules on nanocrystalline semiconductor films.[15] In our model, we took into account the reorganization energy $\lambda_v$ due to the intramolecular vibration of sensitizer dyes and the

heterogeneity $\sigma_{site}$ of the energy level of the surface, both of which were ignored in the previous model.[25] For various dyes adsorbed on ZnO nanocrystalline films, we succeeded in explaining the experimental results on the injection efficiency by using the parameters $\lambda_v = 0.1$ eV and $\sigma_{site} = 0.1-0.2$ eV. The curve in Figure 7 shows the results based on our model with these values of $\lambda_v = 0.1$ eV and $\sigma_{site} = 0.2$ eV. Clearly, the model quantitatively fits the experimental results obtained here. In the present study, however, there are no experimental results near $-\Delta G = 0$ eV and therefore we cannot estimate $\lambda_v$ and $\sigma_{site}$ directly from the results.

As shown in Figure 7, a small amount of excited N3 on $ZrO_2$ films can inject electrons into the films. For N3/$ZrO_2$, $-\Delta G$ is positive, so electron injection is not expected if there is no heterogeneity. According to the result based on our model (the solid line in Figure 8), the electron injection efficiency is not zero, because of site heterogeneity. Namely, the result shown in Figure 7 again shows the importance of the heterogeneity of the surface in nanocrystalline films.

**The Relation between the Injection Efficiency and the Solar Cell Performance.** The solar cell performance has been evaluated by using two important experimental values—open circuit voltage $V_{oc}$ and short circuit current $J_{sc}$. In an ideal case, the energy gap between $E_{CB}$ and the redox mediators corresponds to $V_{oc}$. In fact, a good correlation has been found between $E_{CB}$ and $V_{oc}$ in various semiconductor films.[4] Short circuit current $J_{sc}$ is the photocurrent without load in an external circuit. Although solar cells developed so far using a variety of semiconductor films, $TiO_2$-based solar cells show higher values of $J_{sc}$ than those consisting of other materials. The reason for the exceptional high value of $TiO_2$ will be discussed on the basis of the results obtained here.

To understand the process that limits $J_{SC}$, it is necessary to consider the primary processes of dye-sensitized solar cells (Figure 1). To achieve a high $J_{SC}$, the rates of three competitive reactions are important: (1) the injection must be faster than the relaxation of the excited state of the sensitizer dye; (2) the regeneration must be faster than the recombination; and (3) the transport of electrons must be faster than the reaction with molecules in the solution. As we showed, the injection efficiencies from excited N3 dyes to the conduction band of $TiO_2$, ZnO, $Nb_2O_5$, $SnO_2$, and $In_2O_3$ films are very high, suggesting that process (1) is not a limiting process for $J_{SC}$. It has been observed that the regeneration occurs within 100-ns time range[26] in the N3/$TiO_2$ system, and no recombination was observed in any system within a 100-ns time range as shown in Figure 5. The regeneration process is the reaction between the sensitizer dye and the redox mediator molecules; the rate of regeneration is not sensitive to the nature of the semiconductor. For process (3), both the transport and the reaction with the molecules in the solution can be affected by the nature of the semiconductor. Thus, we consider that process (2) is also unimportant; process (3) is the only possible reason ZnO, $Nb_2O_5$, $SnO_2$, and $In_2O_3$ systems exhibit lower $J_{SC}$ than $TiO_2$. Namely, the reaction of the conducting electron with the molecule in the solution is hindered in the $TiO_2$ system. Recently, Tachibana et al. studied the reaction between conducting electrons and $I_2^-$ produced by photoexcitation.[5] The reaction occurs efficiently for the $SnO_2$ system, but no reaction occurs for the $TiO_2$ system. Thus, the suppression of the reaction is a possible reason for high $J_{SC}$ in $TiO_2$.

## Conclusion

We measured the efficiency of electron injection from excited N3 dyes adsorbed on $ZrO_2$, $TiO_2$, ZnO, $Nb_2O_5$, $SnO_2$, and $In_2O_3$ nanocrystalline films. The efficiencies are almost unity except for N3/$ZrO_2$, for which the bottom of the conduction band is located above the LUMO level of the N3 dye. The observed tendency can be explained by the model presented previously. Thus, it should be possible to realize highly efficient dye-sensitized solar cells by using systems that have a positive $-\Delta G$. However, it is known that only N3/$TiO_2$ gives a high performance for dye-sensitized solar cells. This indicates that the electron injection process is not the limiting step for realizing a high performance and the reaction of conducting electron with the molecule in the solution is the key process for achieving high performance.

**Acknowledgment.** This work was supported by the New Energy and Industrial Technology Development Organization (NEDO) and the COE development program, and by Grants-in-Aid for Scientific Research from the Ministry of Education, Culture, Sports, Science, and Technology (MEXT) of Japan.

## References and Notes

(1) Nazeeruddin, M. K.; Kay, A.; Rodicio, I.; Humphry-Baker, R.; Muller, E.; Liska, P.; Vlachopoulos, N.; Grätzel, M. *J. Am. Chem. Soc.* **1993**, *115*, 6382−6390.

(2) Hagfeldt, A.; Grätzel, M. *Chem. Rev.* **1995**, *95*, 49−68.

(3) Arakawa, H. *Proc. of WCPEC-3* **2003**, *IO-B7-03*.

(4) Sayama, K.; Sugihara, H.; Arakawa, H. *Chem. Mater.* **1998**, *10*, 3825−3832.

(5) Tachibana, Y.; Hara, K.; Takano, S.; Sayama, K.; Arakawa, H. *Chem. Phys. Lett.* **2003**, *364*, 297−302.

(6) Keis, K.; Lindgren, J.; Lindquist, S.-E.; Hagfeldt, A. *Langmuir* **2000**, *16*, 4688−4694.

(7) Horiuchi, H.; Katoh, R.; Hara, K.; Yanagida, M.; Murata, S.; Sugihara, H.; Arakawa, H.; Tachiya, M. *J. Chem. Phys. B* **2003**, *107*, 2570−2574.

(8) Keis, K.; Bauer, C.; Boschloo, G.; Hagfeldt, A.; Westermark, K.; Rensmo, H.; Siegbahn, H. *J. Photochem. Photobiol., A* **2002**, *148*, 57−64.

(9) Asbury, J. B.; Hao, E.; Wang, Y.; Ghosh, H. N.; Lian, T. *J. Phys. Chem. B* **2001**, *105*, 4545−4557.

(10) Iwai, S.; Hara, K.; Murata, S.; Katoh, R.; Sugihara, H.; Arakawa, H. *J. Chem. Phys.* **2000**, *113*, 3366−3373.

(11) Bauer, C.; Boschloo, G.; Mukhtar, E.; Hagfeldt, A. *Int. J. Photochem.* **2002**, *4*, 17−20.

(12) Benkö, G.; Myllyperkiö, P.; Pan, J.; Yartsev, A. P.; Sundström, V. *J. Am. Chem. Soc.* **2002**, *105*, 1118−1119.

(13) Furube, A.; Katoh, R.; Hara, K.; Murata, S.; Arakawa, H.; Tachiya, M. *J. Phys Chem. B* **2003**, *107*, 4162−4166.

(14) Hara, K.; Horiuchi, H.; Katoh, R.; Singh, L. P.; Sugihara, H.; Sayama. K.; Murata, S.; Tachiya, M.; Arakawa, H. *J. Phys. Chem. B* **2002**, *106*, 374−379.

(15) Katoh, R.; Furube, A.; Hara, K.; Murata, S.; Sugihara, H.; Arakawa, H.; Tachiya, M. *J. Phys. Chem. B* **2002**, *106*, 12957−12964.

(16) Barbé, C. J.; Arendse, F.; Comte, P.; Jirousek, M.; Lenzmann, F.; Shklover, V.; Grätzel, M. *J. Am. Ceram. Soc.* **1997**, *80*, 3157−3171.

(17) Hara, K.; Horiguchi, T.; Kinoshita, T.; Sayama, K.; Sugihara, H.; Arakawa, H. *Sol. Energy Mater. Sol. Cells* **2000**, *64*, 115−134.

(18) Nazeeruddin, Md. K.; Zakeeruddin, S. M.; Humphry-Baker, R.; Jirousek, M.; Liska, P.; Vlachopoulos, N.; Shklover, V.; Fischer, C.-H.; Grätzel, M. *Inorg. Chem.* **1999**, *38*, 6298−6305.

(19) Tachibana, Y.; Moser, J. E.; Grätzel, M.; Klug, D. R.; Durrant, J. R. *J. Phys. Chem.* **1996**, *100*, 20056−20062.

(20) Haque, S. A.; Tachibana, Y.; Willis, R. L.; Moser, J. E.; Grätzel, M.; Klug, D. R.; Durrant, J. R. *J. Phys. Chem. B* **2000**, *104*, 538−547.

(21) Barzykin, A. V.; Tachiya, M. *J. Phys. Chem.* **2002**, *106*, 4356−4363.

(22) Yoshihara, T.; Katoh, R.; Furube, A.; Murai, M.; Tamaki, T.; Hara, K.; Murata, S.; Arakawa, H.; Tachiya, M. *J. Phys. Chem. B* **2004**, *108*, 2643−2647.

(23) Bhasikuttan, A. C.; Suzuki, M.; Nakashima, S.; Okada, T. *J. Am. Chem. Soc.* **2002**, *124*, 8398−8405.

(24) Benkö, G.; Kallioinen, J.; Korppi-Tommola, J. E. I.; Yartsev, A. P.; Sundström, V. *J. Am. Chem. Soc.* **2002**, *124*, 489−493.

(25) Sakata, T.; Hashimoto, K.; Hiramoto, M. *J. Phys. Chem.* **1990**, *94*, 3040−3045.

(26) Montanari, I.; Nelson, J.; Durrant, J. R. *J. Phys. Chem. B* **2002**, *106*, 12203−12210.